Electronic Supplementary Information

Multicomponent tandem polymerization of alkynes, CO_2, alkyl bromide, and thiol toward functional poly(β-thioacrylate)s

*Mengchao Zhang, Sifan Li, Zhaohui Zhang, and Hongkun Li**

Laboratory of Advanced Optoelectronic Materials, Suzhou Key Laboratory of Novel Semiconductor-Optoelectronics Materials and Devices, State and Local Joint Engineering Laboratory for Novel Functional Polymeric Materials, Jiangsu Engineering Laboratory of Novel Functional Polymeric Materials, College of Chemistry, Chemical Engineering and Materials Science, Soochow University, Suzhou, 215123, China. E-mail: hkli@suda.edu.cn

Table of Contents

(D) in $CDCl_3$. The solvent peaks are marked with asterisks.

Fig. S7 ^1H NMR spectra of monomer **1d** (A), **2** (B), **3** (C) and polymer P**1d**/**2**/**3**/CO_2 (D) in $CDCl_3$. The solvent peaks are marked with asterisks.

Fig. S8 ^{13}C NMR spectra of monomer **1b** (A), **2** (B), **3** (C) and polymer P**1a**/**2**/**3**/CO_2 (D) in $CDCl_3$. The solvent peaks are marked with asterisks.

Fig. S9 ^{13}C NMR spectra of monomer **1c** (A), **2** (B), **3** (C) and polymer P**1c**/**2**/**3**/CO_2 (D) in $CDCl_3$. The solvent peaks are marked with asterisks.

Fig. S10 ^{13}C NMR spectra of monomer **1d** (A), **2** (B), **3** (C) and polymer P**1d**/**2**/**3**/CO_2 (D) in $CDCl_3$. The solvent peaks are marked with asterisks.

Fig. S11 ^1H NMR spectra of P**1a**/**2**/**3**/CO_2 (A), **4** (B) and polymer P**1a**/**2**/**3**/CO_2/**4** (C) in $CDCl_3$. The solvent peaks are marked with asterisks.

Fig. S12 ^1H NMR spectra of P**1b**/**2**/**3**/CO_2 (A), **4** (B) and polymer P**1b**/**2**/**3**/CO_2/**4** (C) in $CDCl_3$. The solvent peaks are marked with asterisks.

Fig. S13 ^1H NMR spectra of P**1c**/**2**/**3**/CO_2 (A), **4** (B) and polymer P**1c**/**2**/**3**/CO_2/**4** (C) in $CDCl_3$. The solvent peaks are marked with asterisks.

Fig. S14 ^1H NMR spectra of P**1d**/**2**/**3**/CO_2 (A), **4** (B) and polymer P**1d**/**2**/**3**/CO_2/**4** (C) in $CDCl_3$. The solvent peaks are marked with asterisks.

Fig. S15 Particle size of P**1a/2/3**/CO_2 in THF/Wate mixtures with different water fractions. Concentration: 10 μM.

Fig. S16 Photographs of P**1a/2/3**/CO_2-doped LCPN film under daylight and UV light.

Fig. S17 Photographs of P**1b–d/2/3**/CO_2@PA6 film under UV light and after removing UV light for different time.

Preparation of LCPN films doped with P1a/2/3/CO_2

A homogeneous mixture of 2-methyl- 1,4-phenylene bis(4-((6-(acryloyloxy)hexyl)oxy)benzoate) (C6M, 473.5 mg), 4-methoxyphenyl 4-((6-(acryloyloxy)hexyl)oxy)benzoate (RM105, 473.5 mg), benzil dimethyl ketal (BDK, 10.0 mg), CA-Acrylate (42.0 mg), and P**1a**/**2**/**3**/CO_2 (1.0 mg) (their molecular structures shown in Chart 1) was ultrasonically dissolved in 2 mL of DCM. The solution was drop-cast onto quartz substrates, followed by solvent evaporation at 85 °C for 3–5 min. After cooling to room temperature, the samples were photopolymerized under 365-nm xenon lamp irradiation (15 W) for 10 s. Finally, frees tanding films were obtained by mechanically delaminating the polymerized layers from the substrate using a blade.

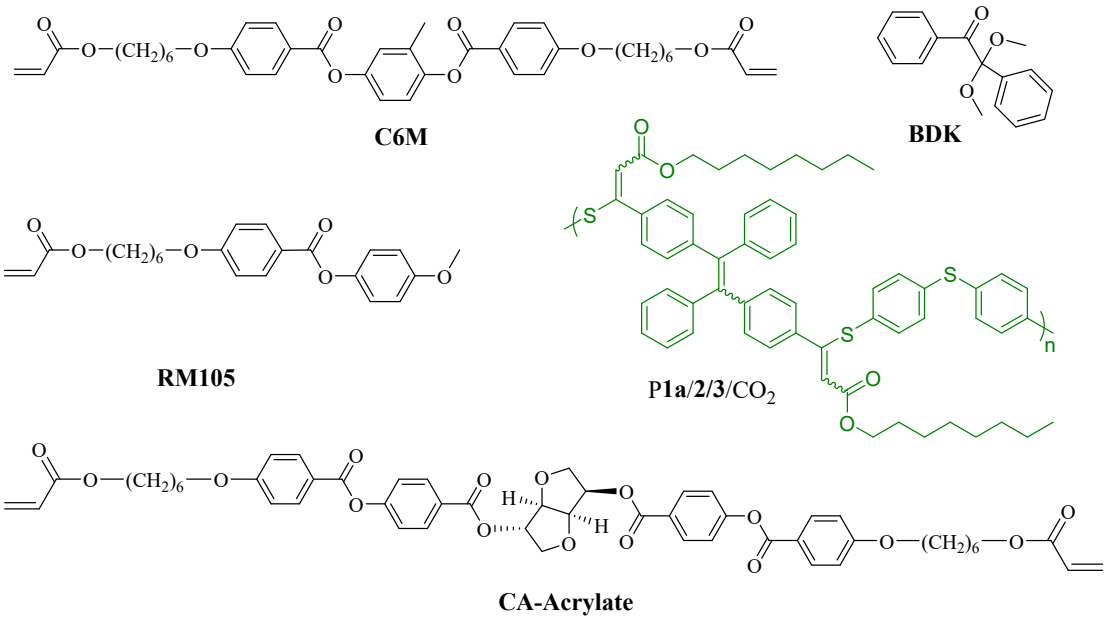

Chart. S1 Molecular structures of the compounds in the polymerizable system.

Table S1 Effect of time on the polymerization of **1a**, CO_2, **2**, and **3**[a]

entry	*t* (h)	M_w[b]	*Đ*[b]	Yield (%)
1	8	6800	1.15	34.7
2	16	9800	1.21	45.4
3	20	10500	1.22	50.4
4	24	11200	1.25	52.6
5	48	12000	1.37	53.5

[a] [**1a**] = 0.4 mol/L, [**1a**]/[Ag_2WO_4]/[Cs_2CO_3]/[**3**] = 1:0.2:6:1, **1a** and **2** were stirred at 80 °C under CO_2 atmosphere in DMAc for 12 h in the presence of Ag_2WO_4 and Cs_2CO_3, followed by reaction with **3** for different time. [b]Estimated by GPC in THF, *Đ* = polydispersity index.

Table S2 Solubility properties of P**1a-d/2/3**/CO_2 in different solvents[a]

Polymer	chloroform	DCM	THF	DMF	DMAc
P**1a/2/3**/CO_2	39	38	41	43	47
P**1b/2/3**/CO_2	35	32	36	33	36
P**1c/2/3**/CO_2	20	19	21	28	33
P**1d/2/3**/CO_2	25	22	28	23	26

[a] Solubility: mg/100 mg, temperature: 20 °C.

Table S3 Solubility properties of P**1a-d**/**2**/**3**/CO_2/**4** in different solvents[a]

Polymer	Chloroform	DCM	THF	DMF	DMAc
P**1a**/**2**/**3**/CO_2/**4**	62	60	54	59	62
P**1b**/**2**/**3**/CO_2/**4**	53	49	48	46	49
P**1c**/**2**/**3**/CO_2/**4**	32	29	34	35	40
P**1d**/**2**/**3**/CO_2/**4**	39	37	35	31	35

[a] Solubiility: mg/100 mg, temperature: 20 °C

Table S4 Comparison on CPL properties of the LCPN films

Sample / Parameter	*S*-TPE-CLC[1]	*R*-PN-TPE/BFN[2]	*S*-PN-TAE/TPEB[3]	*S*-PN-2[4]	PN-TPAP[5]	This work
λ (nm)	485	620	610	550	505	500
g_{max}	0.58	–0.71	0.85	0.70	–0.93	–0.88

[1] B. Ni, Y. Li, W. Liu, B. Li, H. Li and Y. Yang, *Chem. Commun.*, 2021, **57**, 2796.
[2] F. Shi, F. Han, W. Zhang, Y. Yang and H. Li, *Dyes Pigm.*, 2024, **222**, 111910.
[3] F. Shi, L. Xu, J. Zhao, Z. Li, W. Zhang, Y. Yang and H. Li, *Chem. Commun.*, 2024, **60**, 11096.
[4] P. Guan, F. Shi, C. Xu, Y. Yang and H. Li, *J. Phys. Chem. Lett.*, 2025, **16**, 10142.
[5] P. Guan, S. Yu, Y. Yang and H. Li, *Chem. Commun.*, 2025, **61**, 17133.

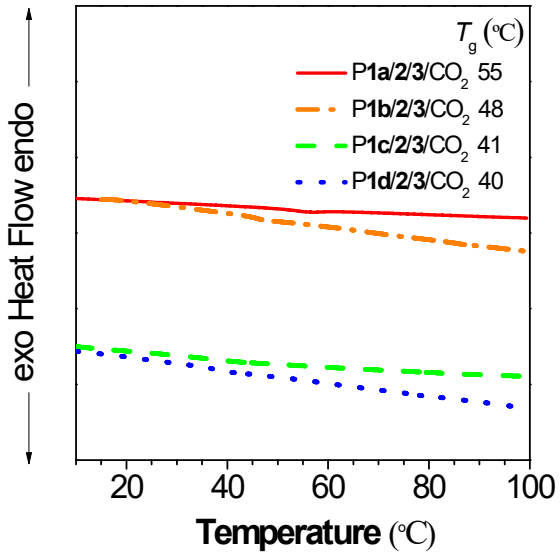

Fig. **S1** DSC Curves of P**1a**–**d**/**2**/**3**/CO_2 under nitrogen at a heating rate of 10 °C min^{-1}.

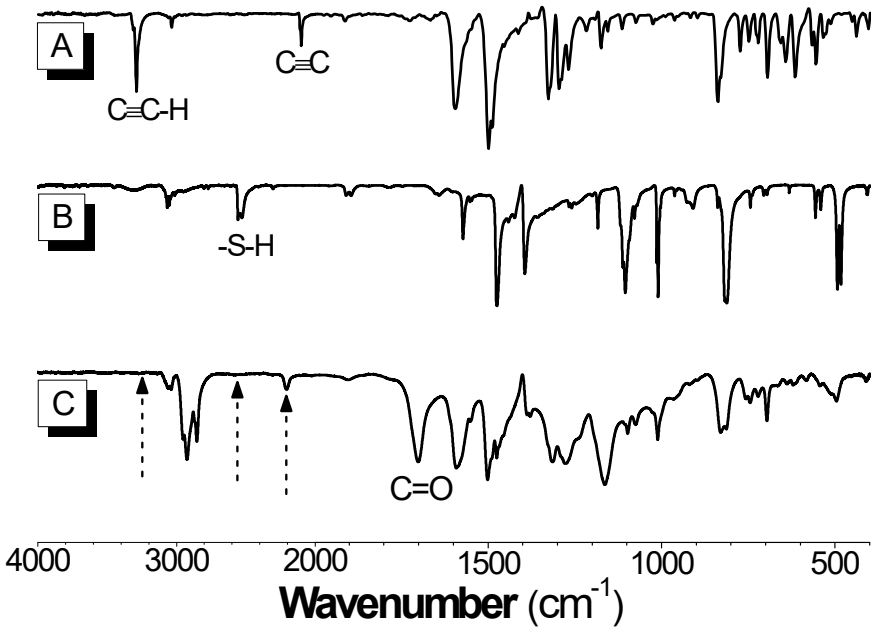

Fig. S2 IR spectra of monomer **1b** (A), **2** (B) and polymer P**1b**/**2**/**3**/CO_2 (C).

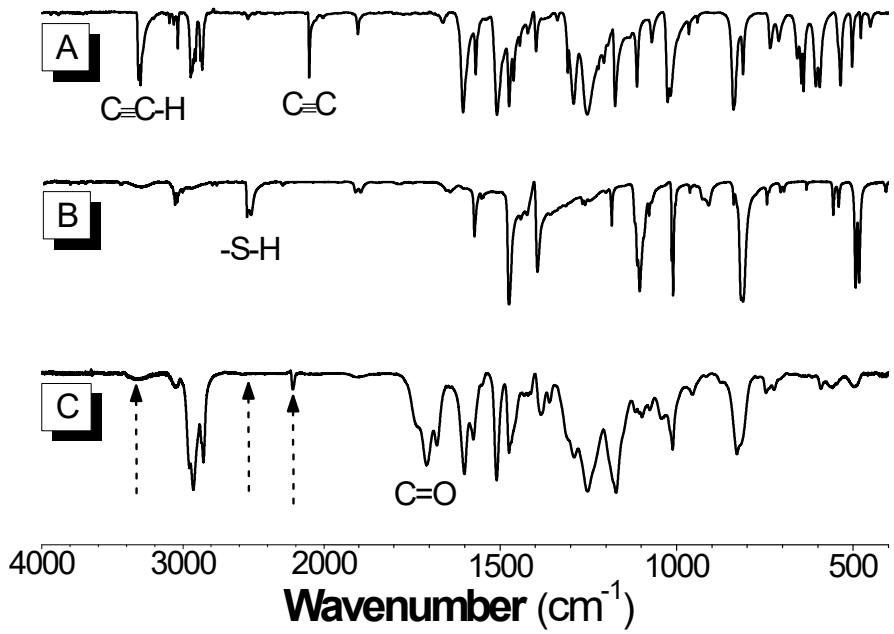

Fig. S3 IR spectra of monomer **1c** (A), **2** (B) and polymer P**1c**/**2**/**3**/CO_2 (C).

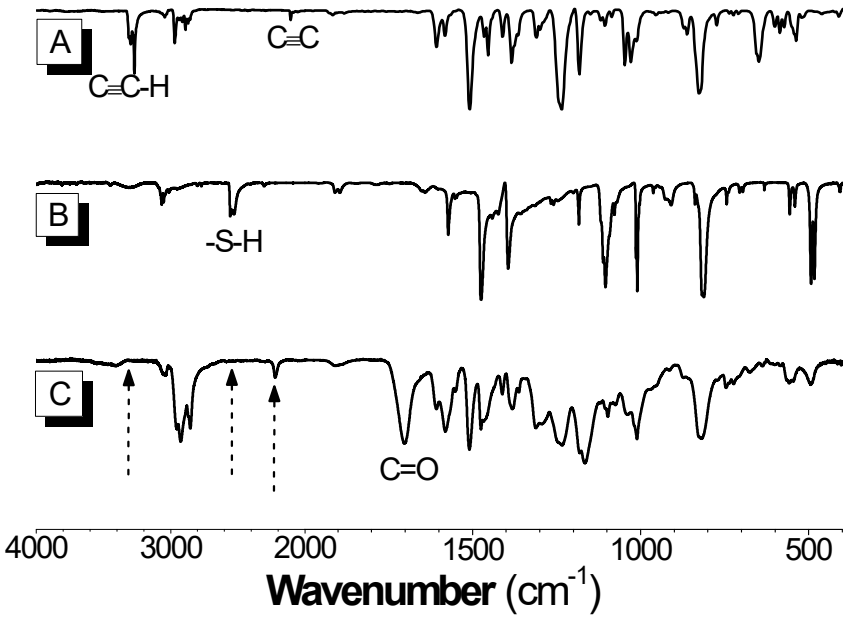

Fig. S4 IR spectra of monomer **1d** (A), **2** (B) and polymer P**1d**/**2**/**3**/CO_2 (C).

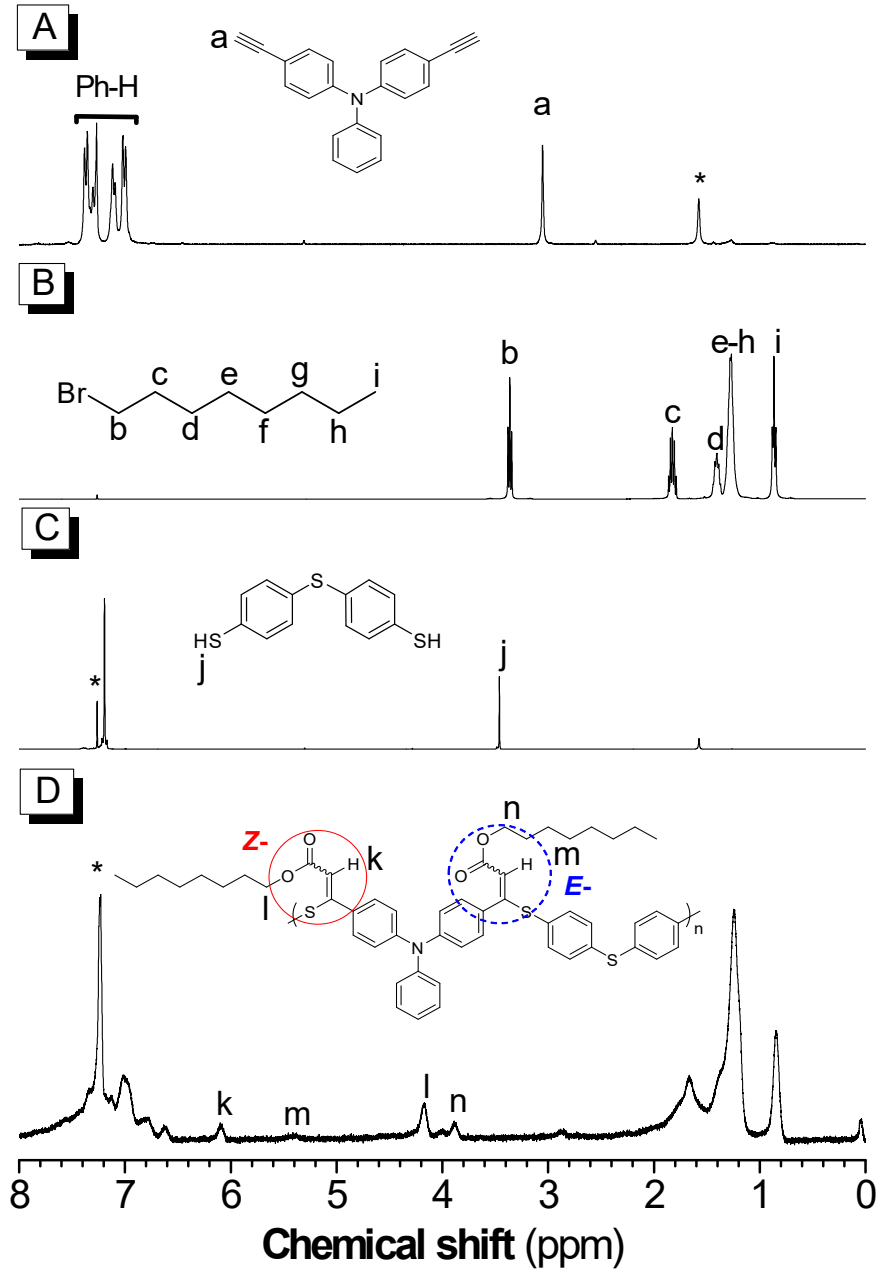

Fig. S5 ^{1}H NMR spectra of monomer **1b** (A), **2** (B), **3** (C) and polymer P**1b**/**2**/**3**/CO_2 (D) in $CDCl_3$. The solvent peaks are marked with asterisks.

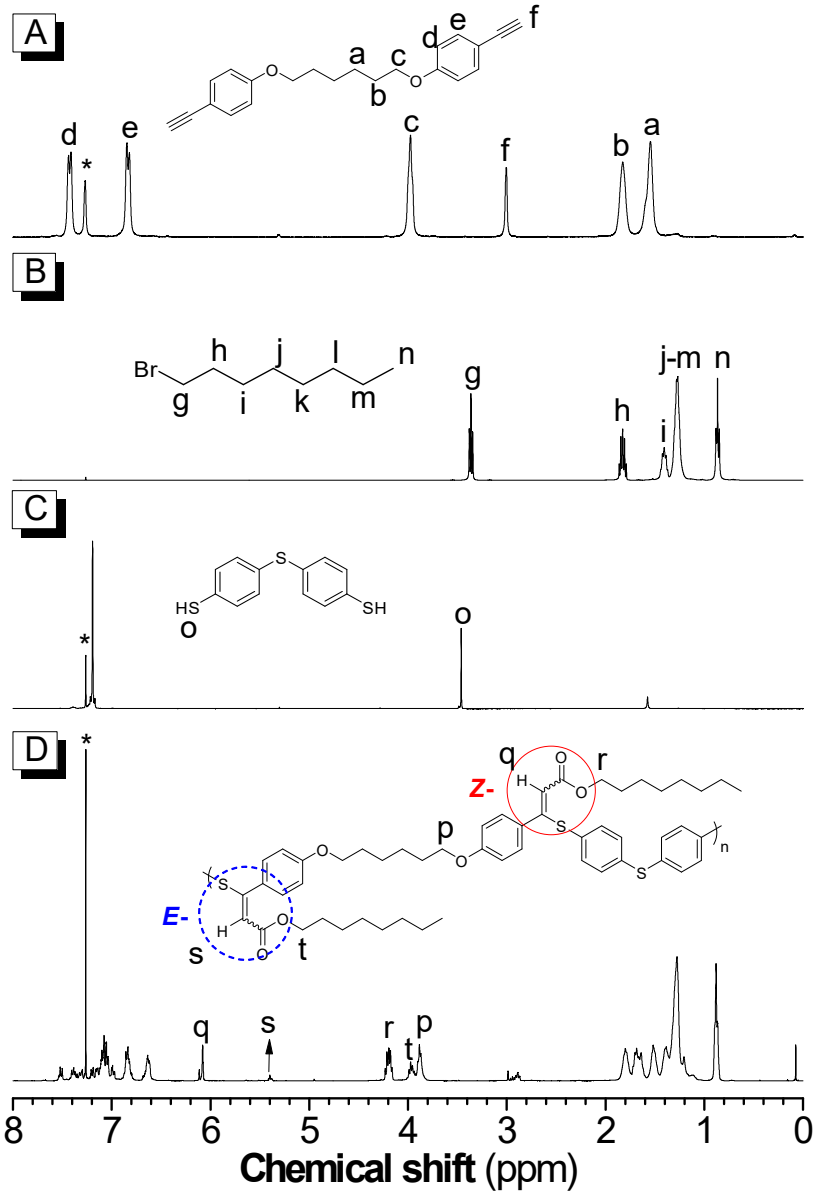

Fig. S6 ^{1}H NMR spectra of monomer **1c** (A), **2** (B), **3** (C) and polymer P**1c**/**2**/**3**/CO_2 (D) in $CDCl_3$. The solvent peaks are marked with asterisks.

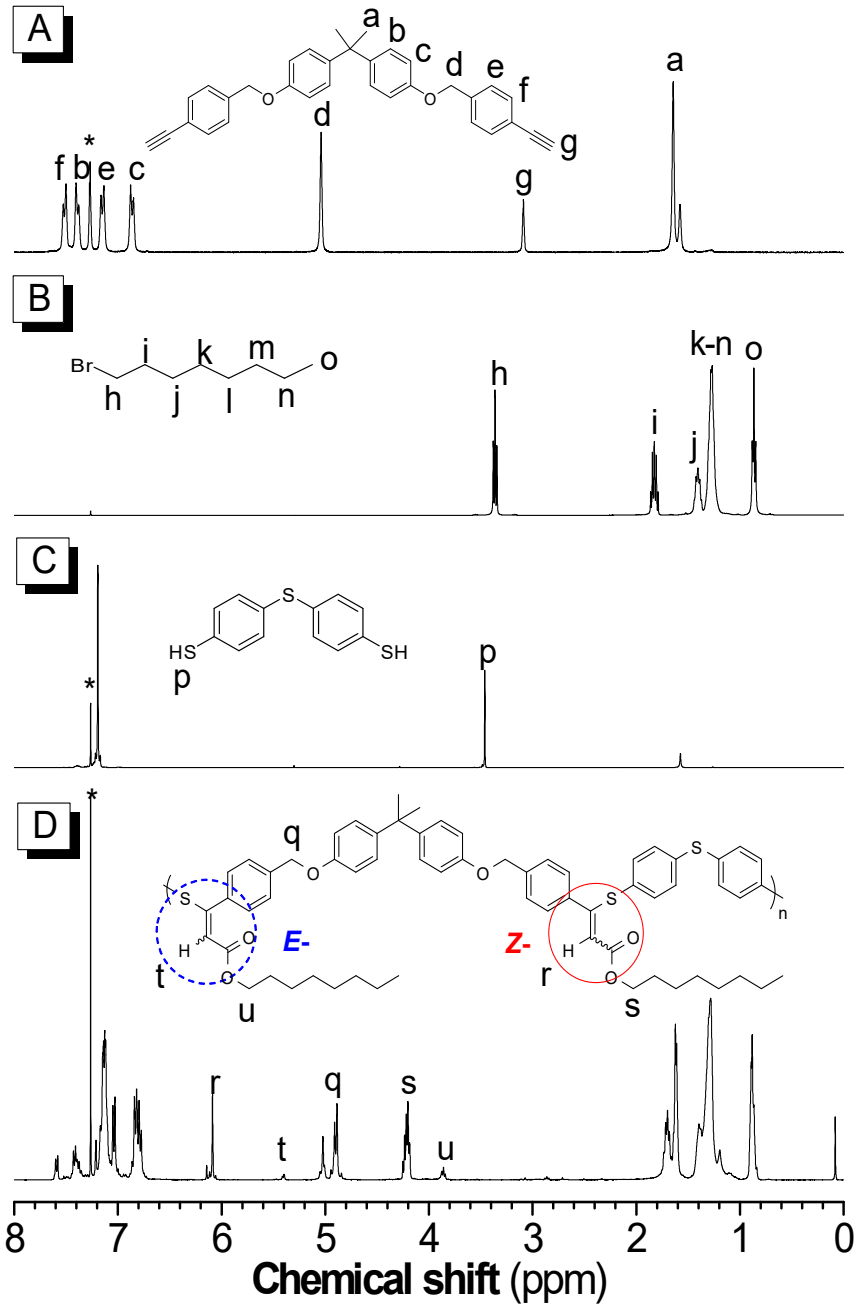

Fig. S7 ^{1}H NMR spectra of monomer **1d** (A), **2** (B), **3** (C) and polymer P**1d**/**2**/**3**/CO_2 (D) in $CDCl_3$. The solvent peaks are marked with asterisks.

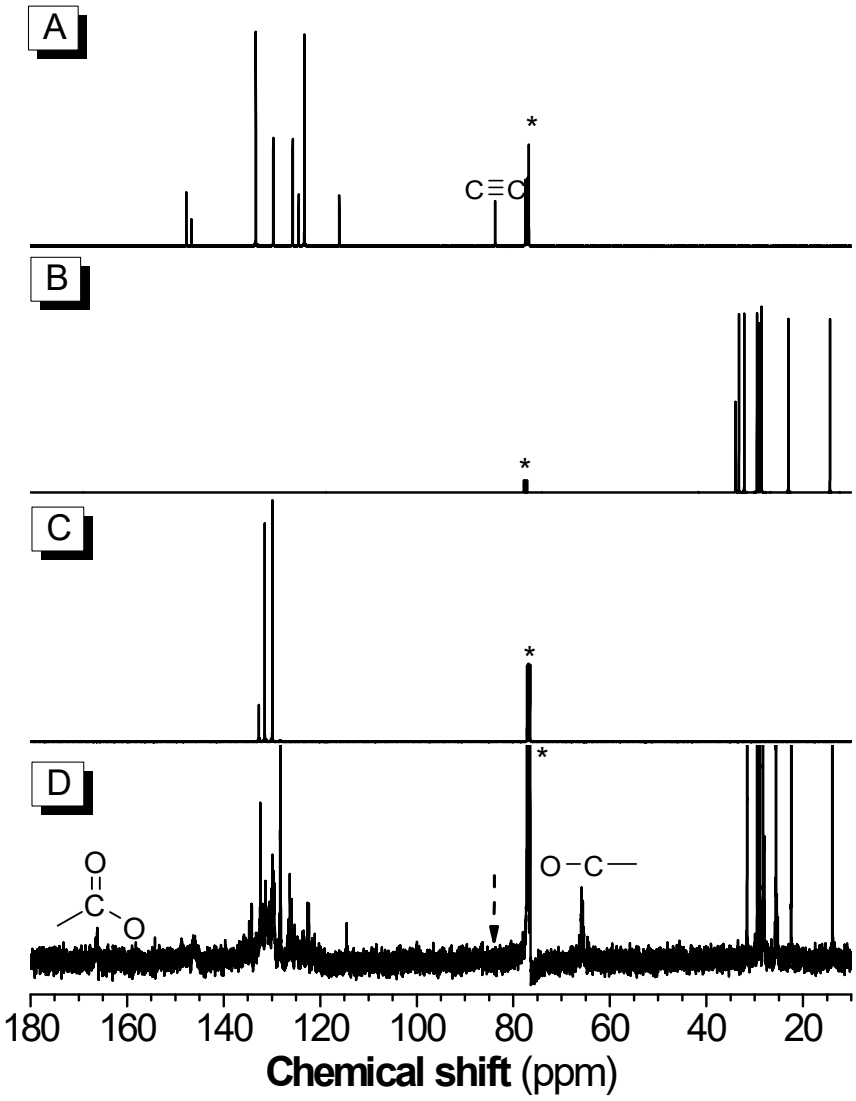

Fig. S8 ^{13}C NMR spectra of monomer **1b** (A), **2** (B), **3** (C) and polymer P**1b**/**2**/**3**/CO_2 (D) in $CDCl_3$. The solvent peaks are marked with asterisks.

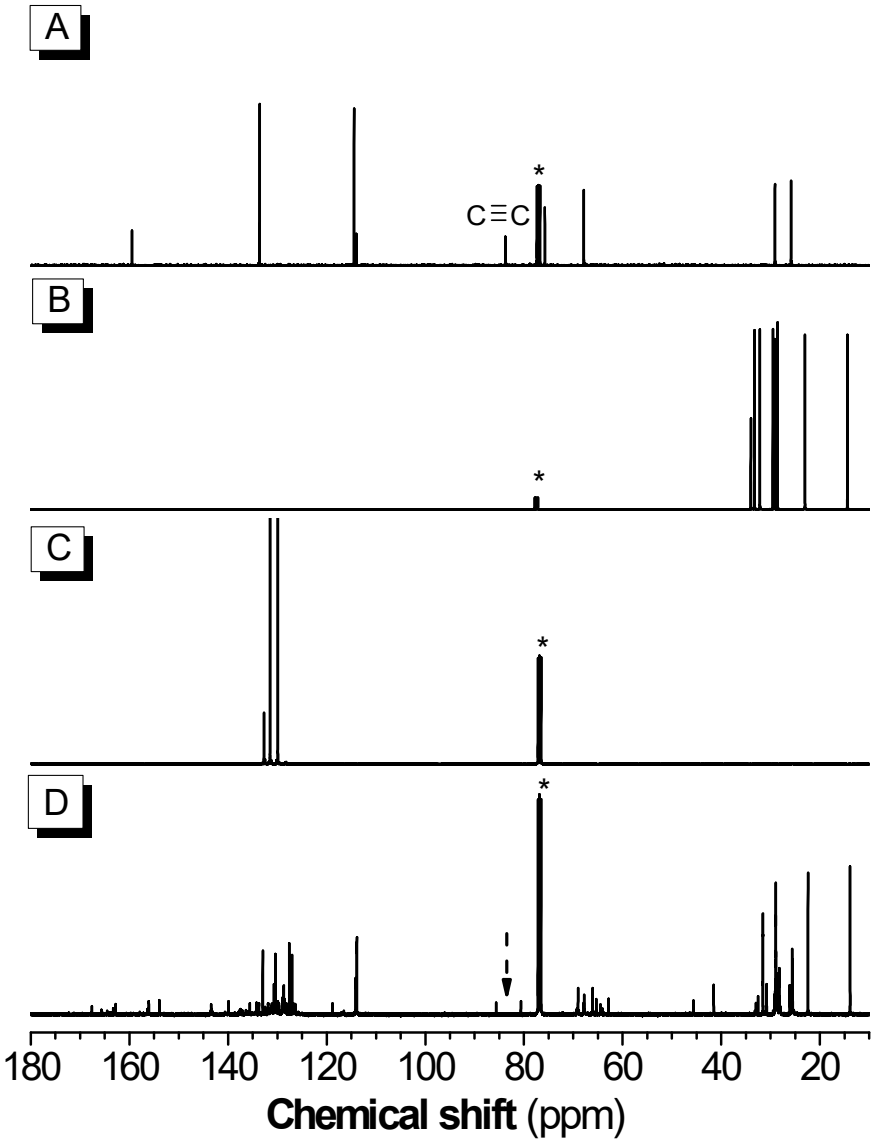

Fig. S9 ^{13}C NMR spectra of monomer **1c** (A), **2** (B), **3** (C) and polymer P**1c**/**2**/**3**/CO_2 (D) in $CDCl_3$. The solvent peaks are marked with asterisks.

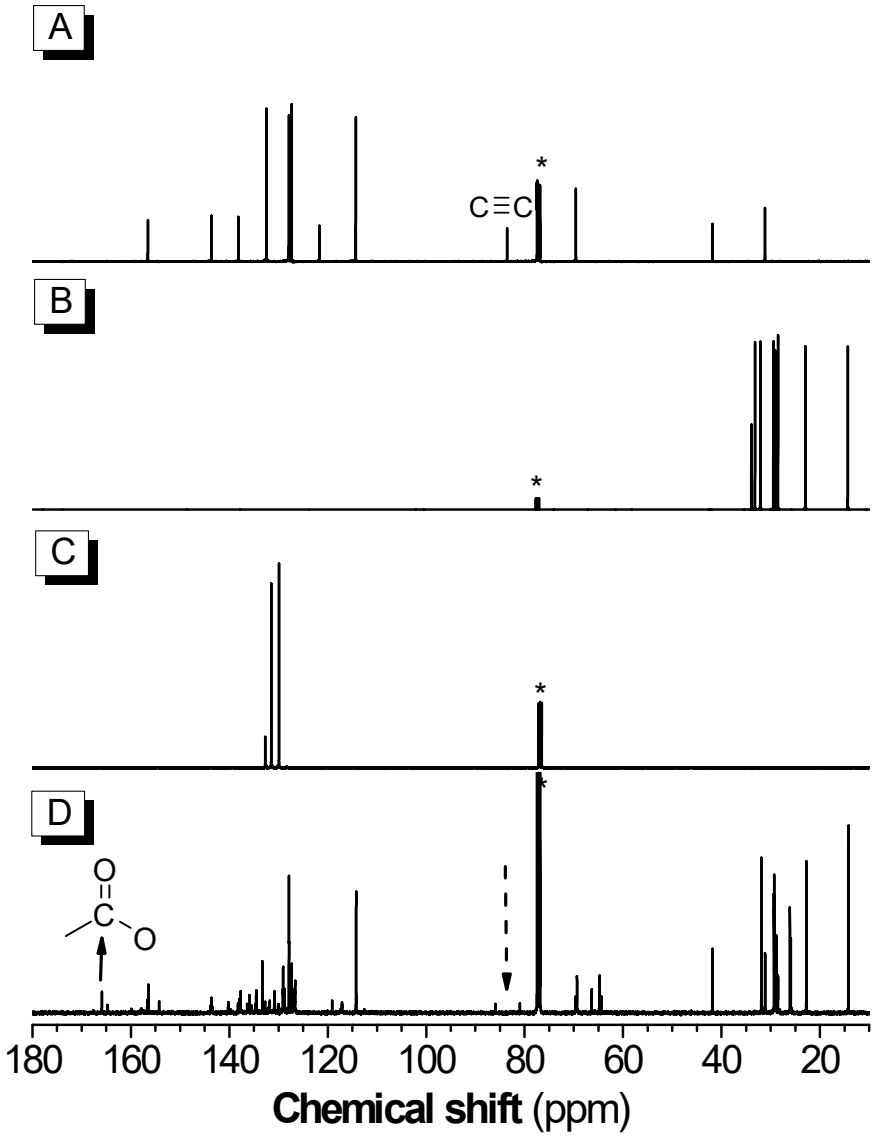

Fig. S10 ^{13}C NMR spectra of monomer **1d** (A), **2** (B), **3** (C) and polymer P**1d**/**2**/**3**/CO_2 (D) in $CDCl_3$. The solvent peaks are marked with asterisks.

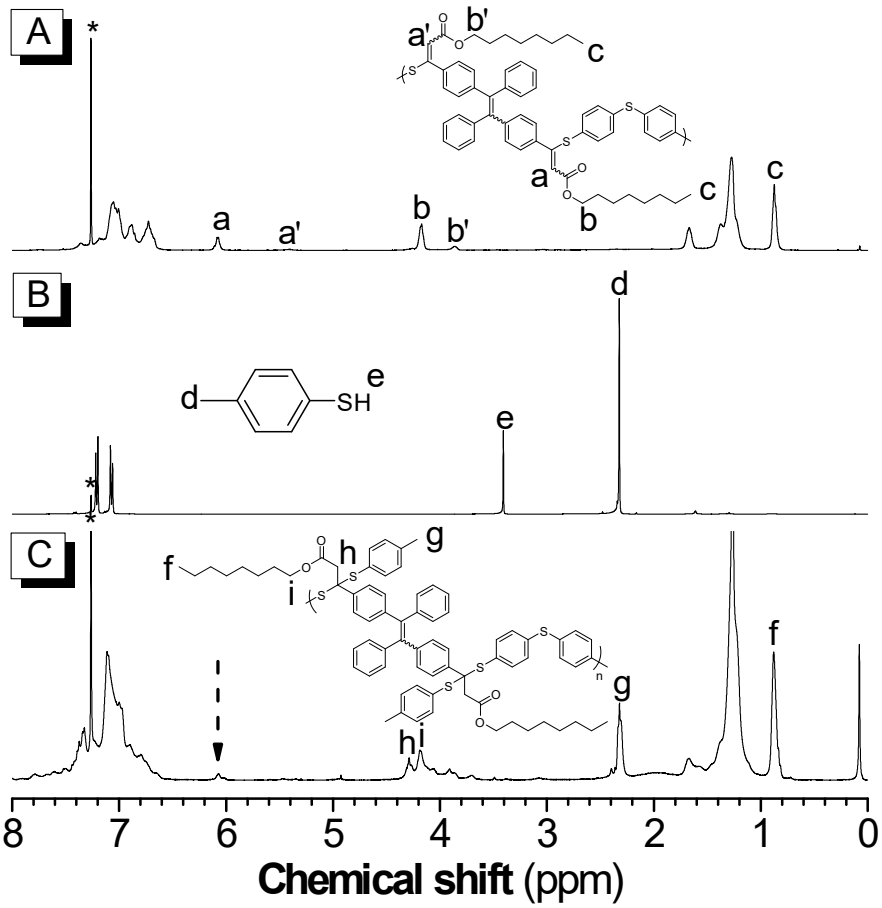

Fig. S11 ^{1}H NMR spectra of P**1a**/**2**/**3**/CO_2 (A), **4** (B) and polymer P**1a**/**2**/**3**/CO_2/**4** (C) in $CDCl_3$. The solvent peaks are marked with asterisks.

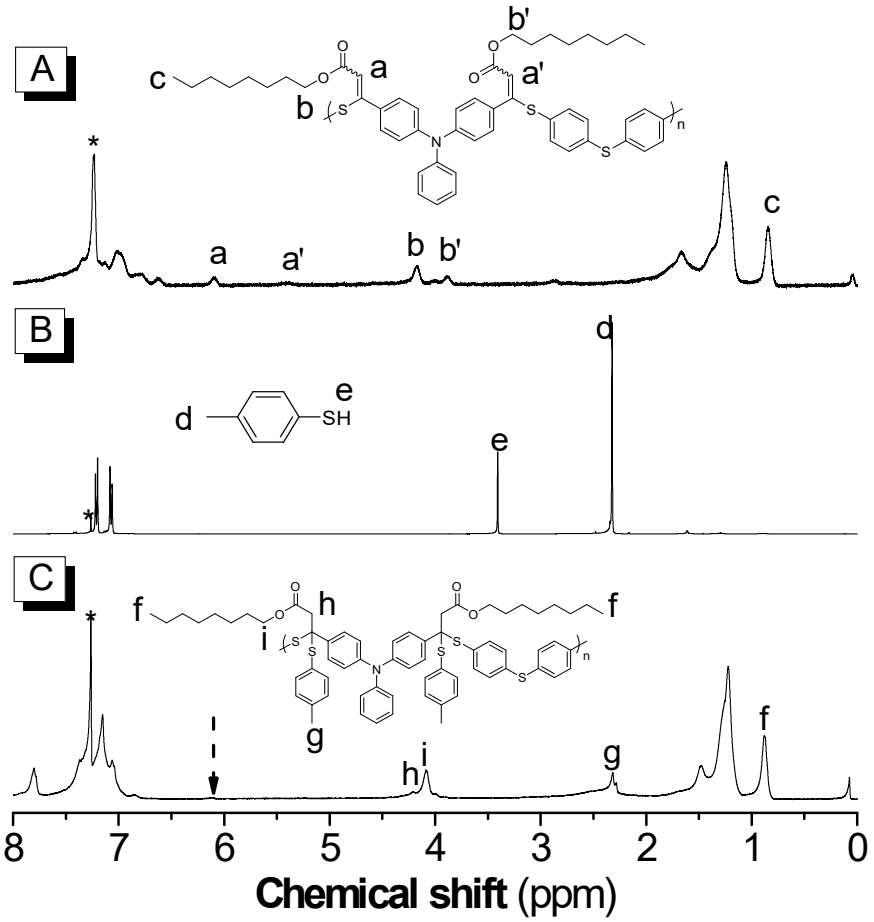

Fig. S12 ^{1}H NMR spectra of polymer P**1b**/**2**/**3**/CO_2 (A), **4** (B) and polymer P**1b**/**2**/**3**/CO_2/**4** (C) in $CDCl_3$. The solvent peaks are marked with asterisks.

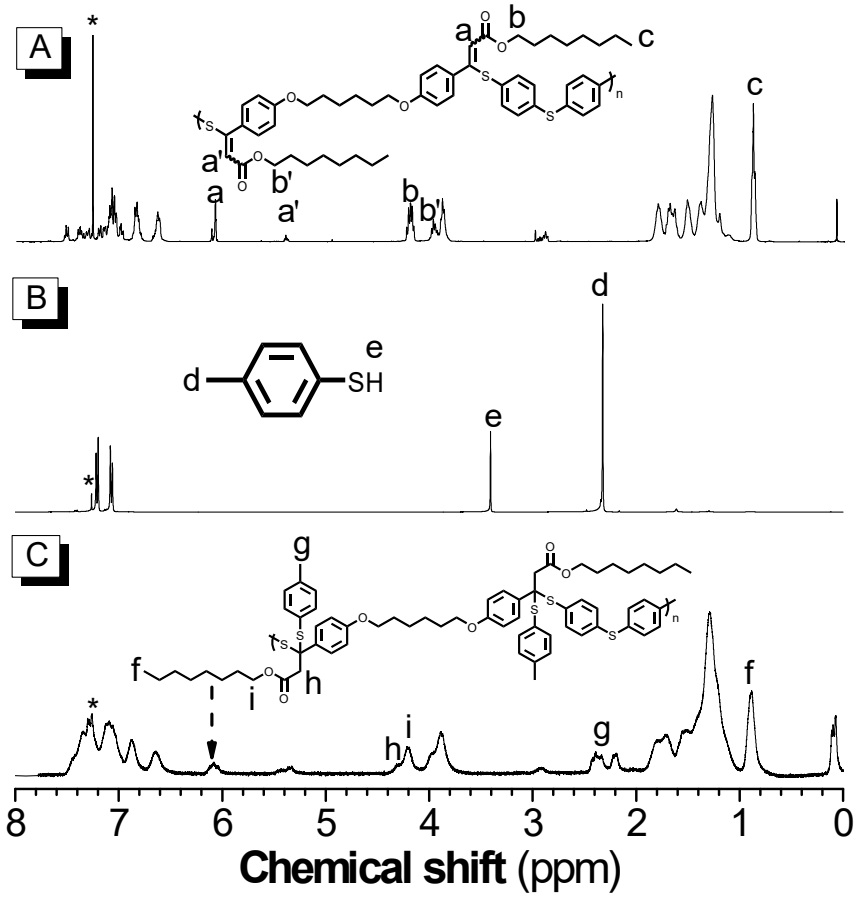

Fig. S13 ^{1}H NMR spectra of P**1c**/**2**/**3**/CO_2 (A), **4** (B) and polymer P**1c**/**2**/**3**/CO_2/**4** (C) in $CDCl_3$. The solvent peaks are marked with asterisks.

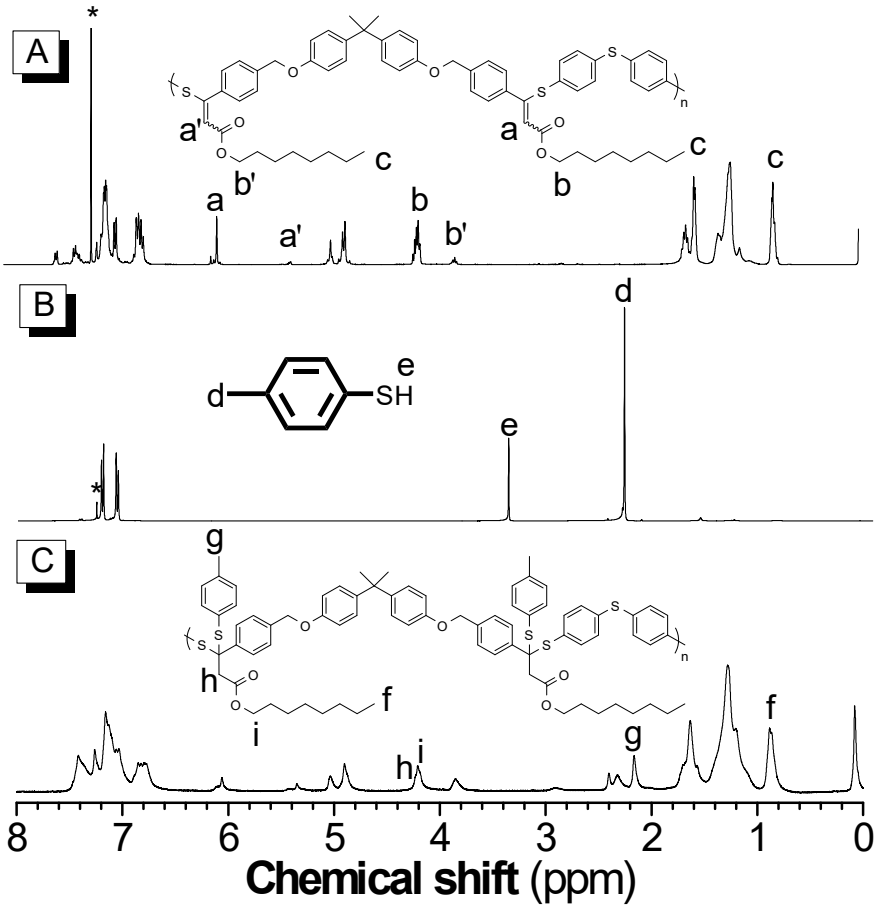

Fig. S14 ^{1}H NMR spectra of P**1d**/**2**/**3**/CO_2 (A), **4** (B) and polymer P**1d**/**2**/**3**/CO_2/**4** (C) in $CDCl_3$. The solvent peaks are marked with asterisks.

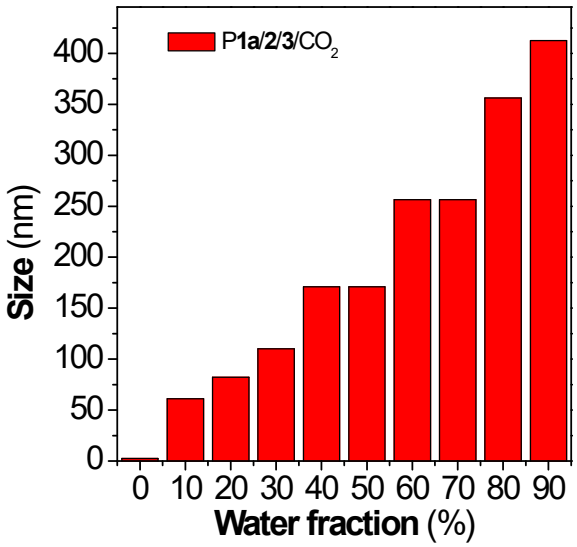

Fig. S15 Particle size of P**1a/2/3**/CO_2 in THF/Wate mixtures with different water fractions. Concentration: 10 μM.

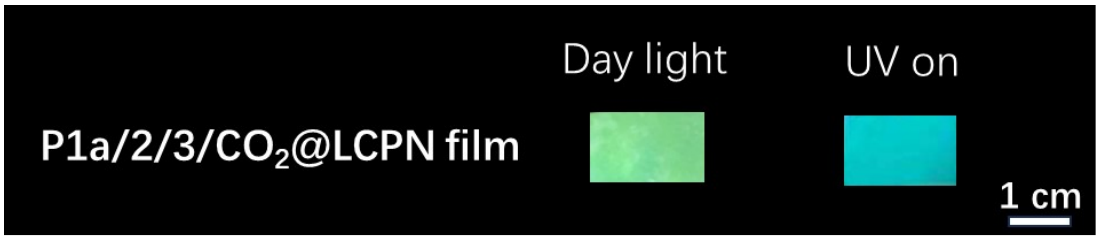

Fig. S16 Photographs of P**1a/2/3**/CO_2-doped LCPN film under daylight and UV light.

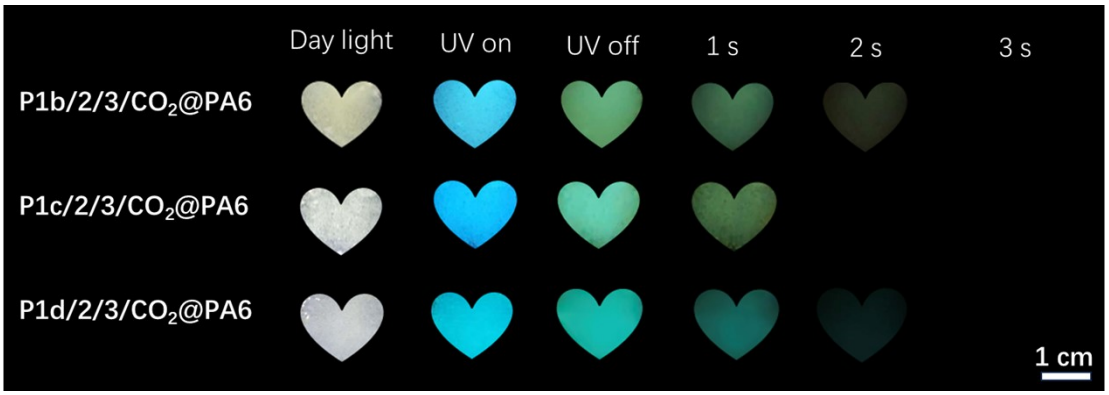

Fig. S17 Photographs of P**1b–d/2/3**/CO_2@PA6 film under UV light and after removing UV light for different time.